



3 4456 0539374 9

ORNL/Sub-79/33200/5

cy. 82

HUGHES

HUGHES AIRCRAFT COMPANY

ELECTRON DYNAMICS DIVISION

FED LIBRARY JAN 29 1982

DEVELOPMENT PROGRAM FOR A 200 kW, CW GYROTRON

FUSION ENERGY DIVISION LIBRARY

J. J. Tancredi, M. Caplan, E. A. Adler, J. J. Sandoval

QUARTERLY REPORT NO. 5 JULY THROUGH SEPTEMBER 1980

Report Prepared by

HUGHES AIRCRAFT COMPANY
Electron Dynamics Division
3100 West Lomita Boulevard
Torrance, California 90509
under
Subcontract No. 53Y-33200C

for
OAK RIDGE NATIONAL LABORATORY
Oak Ridge, Tennessee 37830
operated by
UNION CARBIDE CORPORATION
for the
U.S. DEPARTMENT OF ENERGY
Contract No. W-7405-eng-26

Printed in the United States of America. Available from
National Technical Information Service
U.S. Department of Commerce
5285 Port Royal Road, Springfield, Virginia 22161
NTIS price codes-Printed Copy: A03; Microfiche A01

This report was prepared as an account of work sponsored by an agency of the United States Government. Neither the United States Government nor any agency thereof, nor any of their employees, makes any warranty, express or implied, or assumes any legal liability or responsibility for the accuracy, completeness, or usefulness of any information, apparatus, product, or process disclosed, or represents that its use would not infringe privately owned rights. Reference herein to any specific commercial product, process, or service by trade name, trademark, manufacturer, or otherwise, does not necessarily constitute or imply its endorsement, recommendation, or favoring by the United States Government or any agency thereof. The views and opinions of authors expressed herein do not necessarily state or reflect those of the United States Government or any agency thereof.

DEVELOPMENT PROGRAM FOR A 200 kW, CW GYROTRON

J. J. Tancredi, M. Caplan, E. A. Adler, J. J. Sandoval

QUARTERLY REPORT NO. 5 JULY THROUGH SEPTEMBER 1980

Report Prepared by

HUGHES AIRCRAFT COMPANY
Electron Dynamics Division
3100 West Lomita Boulevard
Torrance, California 90509
under
Subcontract No. 53Y-33200C

for
OAK RIDGE NATIONAL LABORATORY
Oak Ridge, Tennessee 37830
operated by
UNION CARBIDE CORPORATION
for the
U.S. DEPARTMENT OF ENERGY
Contract No. W-7405-eng-26

ABSTRACT

The objective of this program is the design and development of a millimeter-wave device to produce 200 kW of continuous-wave power at 60 GHz. The device, which will be a gyrotron oscillator, will be compatible with power delivery to an electron-cyclotron plasma. Smooth control of rf power output over a 17 dB range is required, and the device should be capable of operation into a severe time-varying rf load mismatch.

During this report period, the electrical design of the CW tube was completed. The mechanical design of a collector, capable of providing diagnostic data of the spent beam in S/N 1 was completed. Cold tests of variations of a scaled, X-band cavity were correlated with the calculated results of a cavity computer code.

Parts for the magnetron injection gun were placed on order and gun tooling was designed. A subcontract was placed for a superconducting solenoid.

A 3 MW power supply was dismantled, packaged and shipped from the Kwajalein Missile Range to storage at Hughes, for use in CW testing at a later date.

During the latter part of this report period, a specific interim goal was imposed by ORNL, to provide for a demonstration of a 200 kW, 60 GHz gyrotron capable of 100 ms pulses, by December 31, 1981. The imposition of this interim goal has led to establishing a modified gyrotron design, based on a considerably smaller collector than that required for a CW tube.

TABLE OF CONTENTS

<u>Section</u>		<u>Page</u>
1.0	INTRODUCTION	1
2.0	PROGRESS	4
2.1	Magnetron Injection Gun	4
2.2	Anode Drift Region	4
2.3	Superconducting Solenoid	6
2.4	Cavity	6
	2.4.1 Cold Tests	6
	2.4.2 Cavity Designs	10
	2.4.3 Threshold Analysis	16
	2.4.4 Final Cavity Design	20
2.5	917H (CW) Collector	20
2.6	919H (100 ms) Collector	21
2.7	917H CW Output Window	22
2.8	919H (100 ms) Output Window	22
2.9	Power Supplies	29
	2.9.1 Short Pulse Power Supply	29
	2.9.2 Medium Pulse Power Supply	29
	2.9.3 CW Power Supply	29
2.10	Gyrotron Facility	30
3.0	SCHEDULE	32

LIST OF ILLUSTRATIONS

<u>Figure</u>	<u>Page</u>
1-1 Schematic of gyrotron oscillator showing applied magnetic field and the rf field and gain in the cavity.	3
2.2-1 Magnetic field, tunnel radius required for TE ₂₂ mode interaction and actual tunnel radius in the anode drift region.	5
2.3-1 Totally enclosed, reduced length cryostat permitting maximum access to Gyrotron.	7
2.4.1-1 Q_{EXT} vs angle.	9
2.4.1-2 Gyrotron cold test TE ₀₂₁ mode profile measurement.	11
2.4.1-3 Measured profile vs computer result.	12
2.4.2-1 Phase bunching of hollow electron beams.	13
2.4.2-2 Cavity configuration A.	14
2.4.2-3 Efficiency analysis of configuration A.	15
2.4.2-4 Cavity configuration B.	17
2.4.2-5 Efficiency analysis of configuration B.	18
2.4.3-1 Start-up threshold analysis.	19
2.7-1 Double-Disc Window - preliminary sketch.	23
2.7-2 Calculated VSWR of double disc window, with dielectric coolant in the gap between windows. (Window thickness = 0.117").	24
2.7-3 Calculated VSWR of double disc window, with dielectric coolant in the gap between windows. (Window thickness = 0.118").	25
2.8-1 Calculated VSWR of single BeO window, no gap.	26
2.8-2 Mechanical design of single disc window.	28
2.10-1 Preliminary facility layout.	31

1.0 INTRODUCTION

The technical baselines for the gyrotron and the associated power supply are shown in Table I. In the gyrotron, which is shown schematically in Figure 1-1, the electrons are formed into a hollow beam by a magnetron-injection electron gun with a considerable amount of their energy in rotation. A gradually rising magnetic field compresses the beam in diameter and at the same time increases the orbital energy according to the theory of adiabatic invariants until approximately 2/3 of the beam energy is in rotation and the rotational frequency is 60 GHz; at this point the magnetic field becomes uniform and the beam enters a quasi-optical open cavity where the spinning electrons interact with the eigen mode of the cavity. The rf energy builds up at the expense of the rotational energy of the dc beam. The spent beam enters the region of decreasing magnetic field, undergoes decompression and impinges on the collector. The latter also functions as the output waveguide. In order to handle the power in the spent beam and the power dissipation in the window, the output waveguide tapers up from the cavity diameter to an appropriate value.

During this report period, progress was made in the following areas:

- Magnetron Injection Gun
- Anode Drift Region
- Superconducting Solenoid
- Cavity
- Collector
- Window
- Power Supplies
- Gyrotron Facility

The CW gyrotron being developed is the 917H. During the latter part of this report period, a specific interim goal was established by ORNL, which requires the demonstration of a 100 ms device by December 31, 1981. Although peak heating effects due to long pulse lengths are considerable, the collector for a 100 ms gyrotron does not need to be as long, nor as overmoded, as the collector

for the CW tube. Consequently, a revised collector design was initiated, and this new 100 ms gyrotron is called the 919H.

TABLE I

<u>The Gyrotron</u>	
Frequency	60 GHz
Power out	200 kW RF
Electronic efficiency	35%
Beam voltage	70-80 kV
Beam current	7.0-8.0 A
Modulation voltage	23 kV
Magnetic field	23.0 kG
Transverse to longitudinal velocity ratio	1.5 - 2.0
<u>The Power Supply</u>	
Voltage rating	100 kV dc
Current rating	10 A
Anode supply voltage	0-35 kV dc
Anode supply current	<20.0 mA
Heater supply voltage	0-15 V, ac
Heater supply current	15 A
<u>Operating Modes:</u>	
1.	10 μ s pulse length
2.	1 ms - 100 ms pulse length
3.	30 s to cw

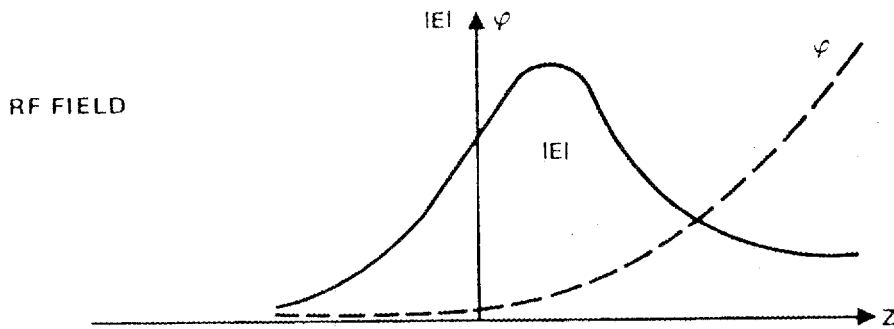
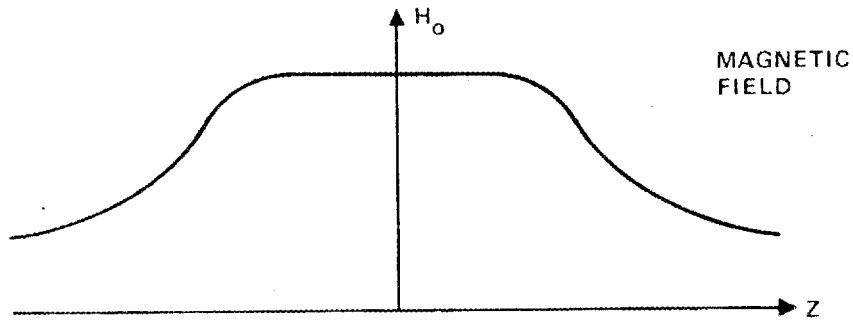
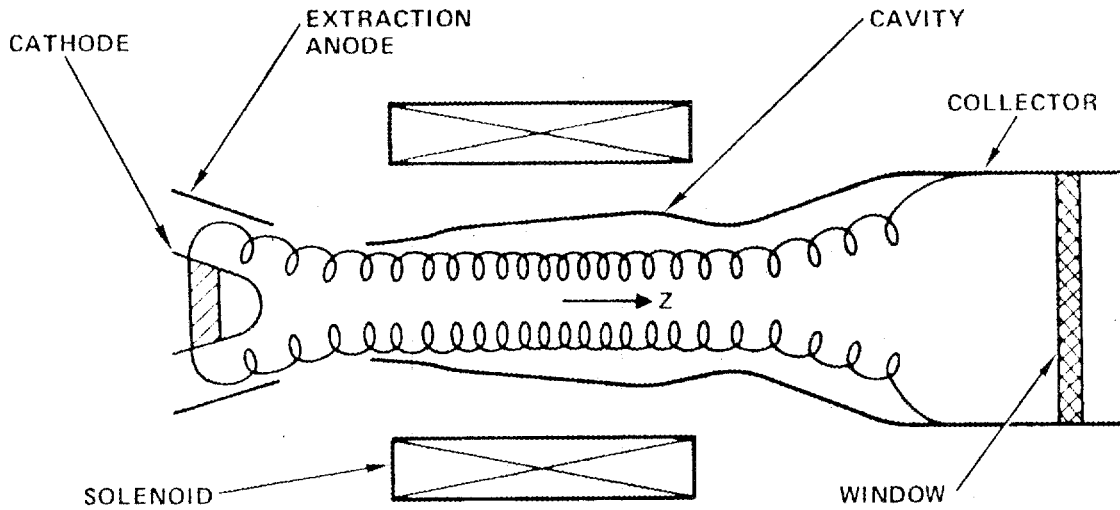


Figure 1-1 Schematic of gyrotron oscillator showing applied magnetic field and the rf field and gain in the cavity.

2.0 PROGRESS

2.1 MAGNETRON INJECTION GUN

The mechanical design of the magnetron injection gun shown in the last report¹ was completed. Parts were placed on order and are expected to be received during the last quarter of 1980. Tooling for assembling this gun has been designed, and placed on order.

The first gun is expected to be assembled by December 1980, and a back-up gun by January 1981.

2.2 ANODE DRIFT REGION

The region between the second anode and the cavity must be carefully designed in order to eliminate the possibility of gyrotron-type interaction in that region. The beam is undergoing adiabatic compression and requires a finite axial distance to reach the cathode at the correct radius for the TE_{02} mode. While the optimum magnetic field for the TE_{02} mode is reached only when the beam is in the interaction cavity, the magnetic field is almost optimum for the next closest mode, the TE_{22} , in the drift region. The drift tunnel therefore should be designed in conjunction with the transition magnetic field, to not interact with the TE_{22} mode.

Figure 2.2-1 illustrates the designed magnetic field in the drift region and the tunnel radius which is required for TE_{22} mode interaction. Also shown is the actual tunnel radius which will be used in S/N 1. It can be seen from Figure 2.2-1 that the TE_{22} mode will be cut-off at all points within the anode drift region.

The electrical and mechanical design of this drift region will be completed in the next quarter.

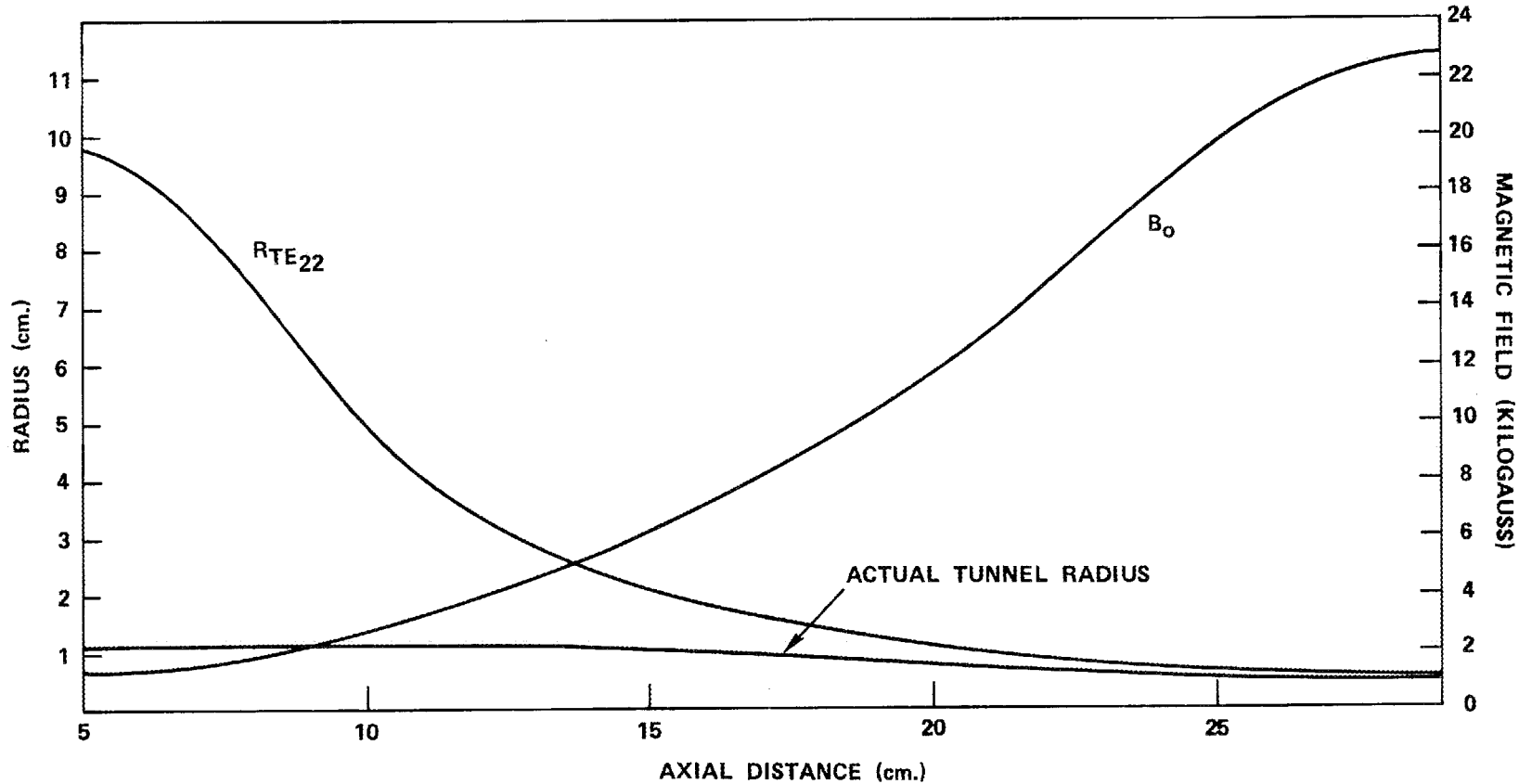


Figure 2.2-1 Magnetic field, tunnel radius required for TE₂₂ mode interaction and actual tunnel radius in the anode drift region.

2.3 SUPERCONDUCTING SOLENOID

Bids were solicited from four vendors for the superconducting solenoid and power supplies, as designed in the last quarter.¹ Two bids were received, and the successful bidder was Magnetic Corporation of America, Waltham, MA. Their cryostat design is shown schematically in Figure 2.3-1.

The desirable uniqueness of this design is that the top of the cryostat is free from obstructions which could interfere with the gyrotron. Connections for eight coils and fill tubes are all serviced from a 45° angle arm.

Delivery of this solenoid is expected by February 1981.

2.4 CAVITY

An X-band cavity was constructed and evaluated. This cold test cavity was comprised of an input section which could be straight or have variable tapers, as well as variable length. In addition, the cavity output horn could have a variable angle. From these cold tests, 60 GHz cavities were designed and evaluated on the computer.

2.4.1 Cold Tests

Cold test measurements at 10.0 GHz were performed to determine external Q factors and mode profiles. The TE_{021} modes were excited using correctly oriented inductive coupling loops attached to coax probes inserted into the side walls of the cavity. Table 2.4.1-1 gives the results of some of these measurements and compares these with values calculated from the Hughes cavity code.² The strong decrease of Q_{Ext} with the input taper angle (θ_1) and somewhat oscillatory dependence of Q_{Ext} on the output taper angle (θ_2) predicted by theory was verified qualitatively and in many cases good quantitative agreement was obtained. This is illustrated in Figure 2.4.1-1.

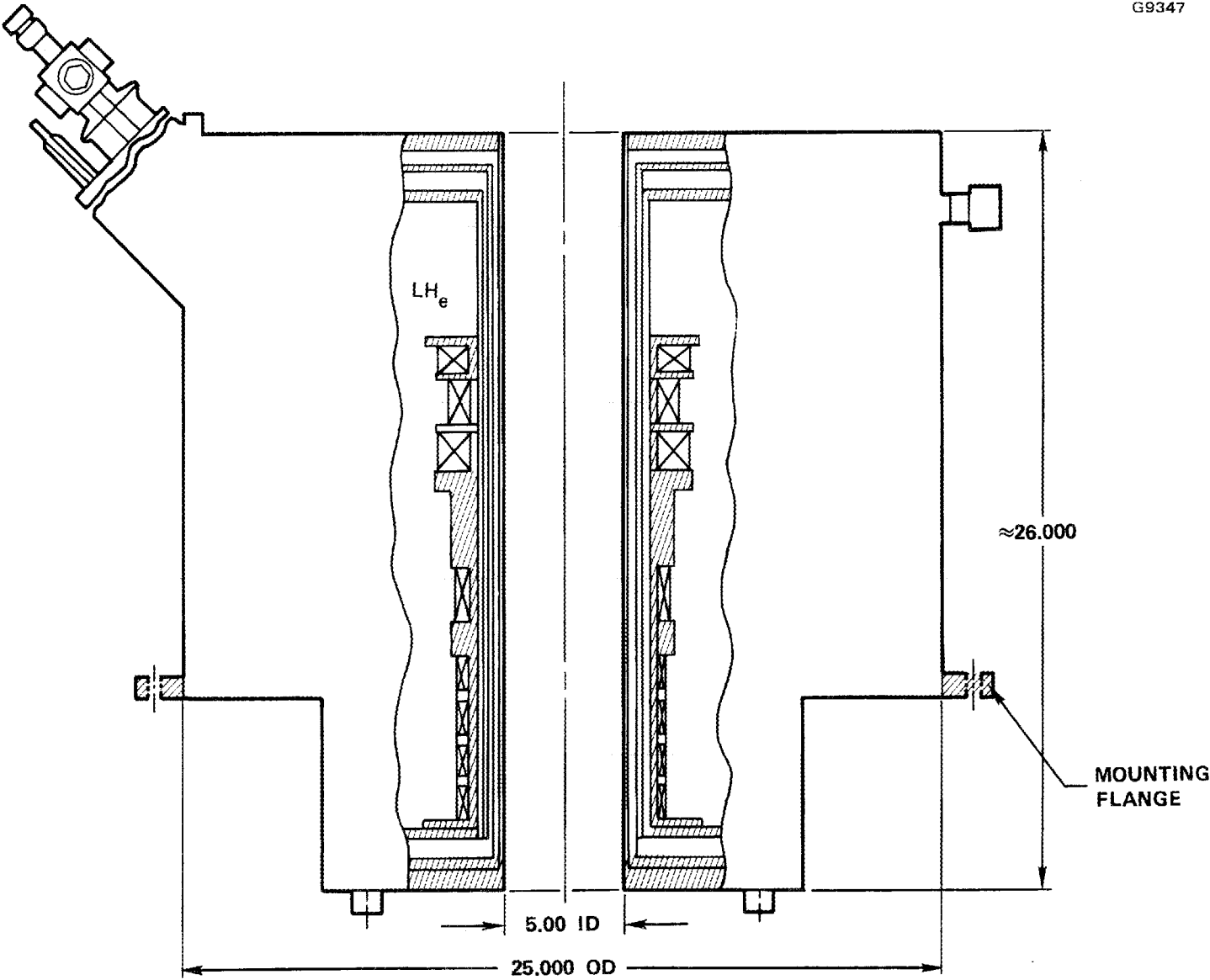


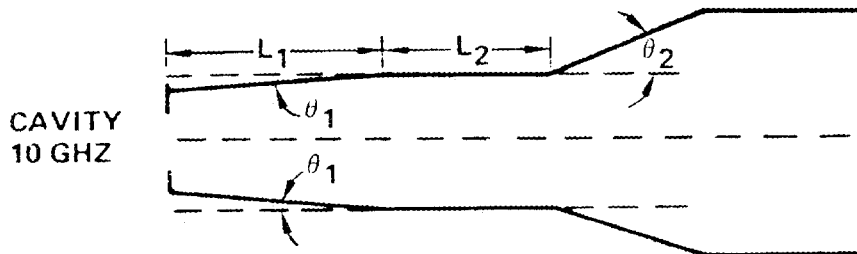
Figure 2.3-1 Totally enclosed, reduced length cryostat permitting maximum access to Gyrotron.

TABLE 2.4.1-1
Q MEASUREMENTS

$$Q_{\text{Ext}} = (1/Q_{\text{TOT}} - 1/Q^{\circ})^{-1}$$

$Q^{\circ} = \text{Unloaded } Q \sim 6000$

L_1 (CM)	L_2 (CM)	θ_1	θ_2	$Q_{\text{Lab}}^{\text{Tot}}$	$Q_{\text{Lab}}^{\text{Ext}}$	$Q_{\text{Theory}}^{\text{Ext}}$
12.8	12.40	0°	15°	1685	2342	2190
12.8	12.40	0°	30°	2655	4762	3582
12.8	12.40	0.47°	10°	737	840	979
12.8	12.40	0.47°	15°	645	722	778
12.8	12.40	0.47°	30°	886	1039	1195
12.8	12.40	1.04°	15°	548	603	621
12.8	12.40	1.04°	30°	760	870	949
12.8	12.40	1.42°	15°	231	240	575
12.8	7.48	0°	10°	711	806	-
12.8	7.48	0°	15°	981	1172	1253
12.8	7.48	0°	30°	847	986	-
12.8	7.48	0°	30° + Iris	2115	3266	-
12.8	7.48	0.47°	15°	372	296	325
12.8	7.48	0.47°	30°	434	467	650



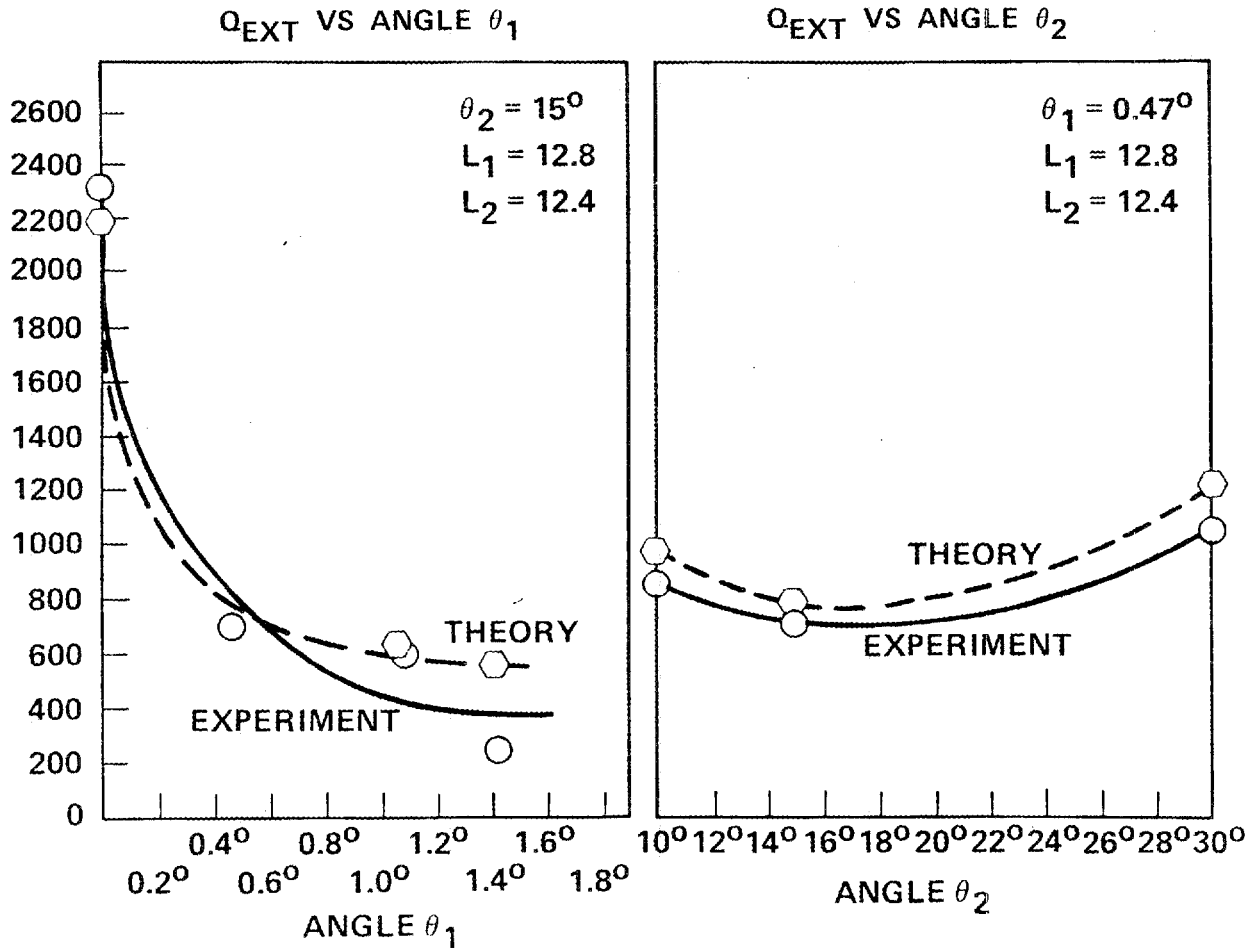


Figure 2.4.1-1 Q_{EXT} vs angle.

The input taper angle, apart from greatly lowering Q_{Ext} also narrows the mode structure and shifts the mode peak forward, giving the mode a gaussian rather than a sinusoidal shape. This was verified by frequency shift measurements and theory as illustrated in Figures 2.4.1-2 and 2.4.1-3. Varying the output taper angle allows Q_{Ext} to vary up to 30%, but leaves the internal mode structure unchanged.

There are several explanations for the disagreement between cold test measurements and theory based on single mode analysis. The TM_{121} mode is degenerate with the TE_{021} mode and can easily be excited. The resultant mode, which is a linear combination of TE_{021} and TM_{121} appears to have a larger half width and hence a lower Q_{Ext} than the TE_{021} mode alone. The finite size probes also cause mode distortion and place extra loading on the cavity. In general, mode coupling is always present due to a varying cavity radius and wall loss, creating other channels by which RF can leak out of the cavity. In addition, at low values of Q_{Ext} , separation of the desired mode from adjacent modes is more difficult. Finally, there is some mismatch between the final output horn and free space, causing reflection and thus distorting the Q measurement.

2.4.2 Cavity Designs

Final cavity designs were arrived at using computer simulations of the beam interaction (Figure 2.4.2-1) with guidance provided by cold test measurements. The following set of cavities at 60.0 GHz were sent out to be fabricated:

Cavity Configuration A

Figure 2.4.2-2 shows the dimensions for cavities #1, 2, and 3 all having input taper angles of 0.47° with length to radius ratio of 6:1 and a gaussian shaped mode profile (verified from cold test, Figure 2.4.1-3). These cavities are to be operated in a flat magnetic field, and are predicted to have an optimized power of at least 200 kW output if Q_{Ext} lies between 200 and 596 (Figure 2.4.2-3). The beam voltage is assumed to be 70 kV, beam current 8 amps and perpendicular to parallel velocity is 1.5. Present cold test data at

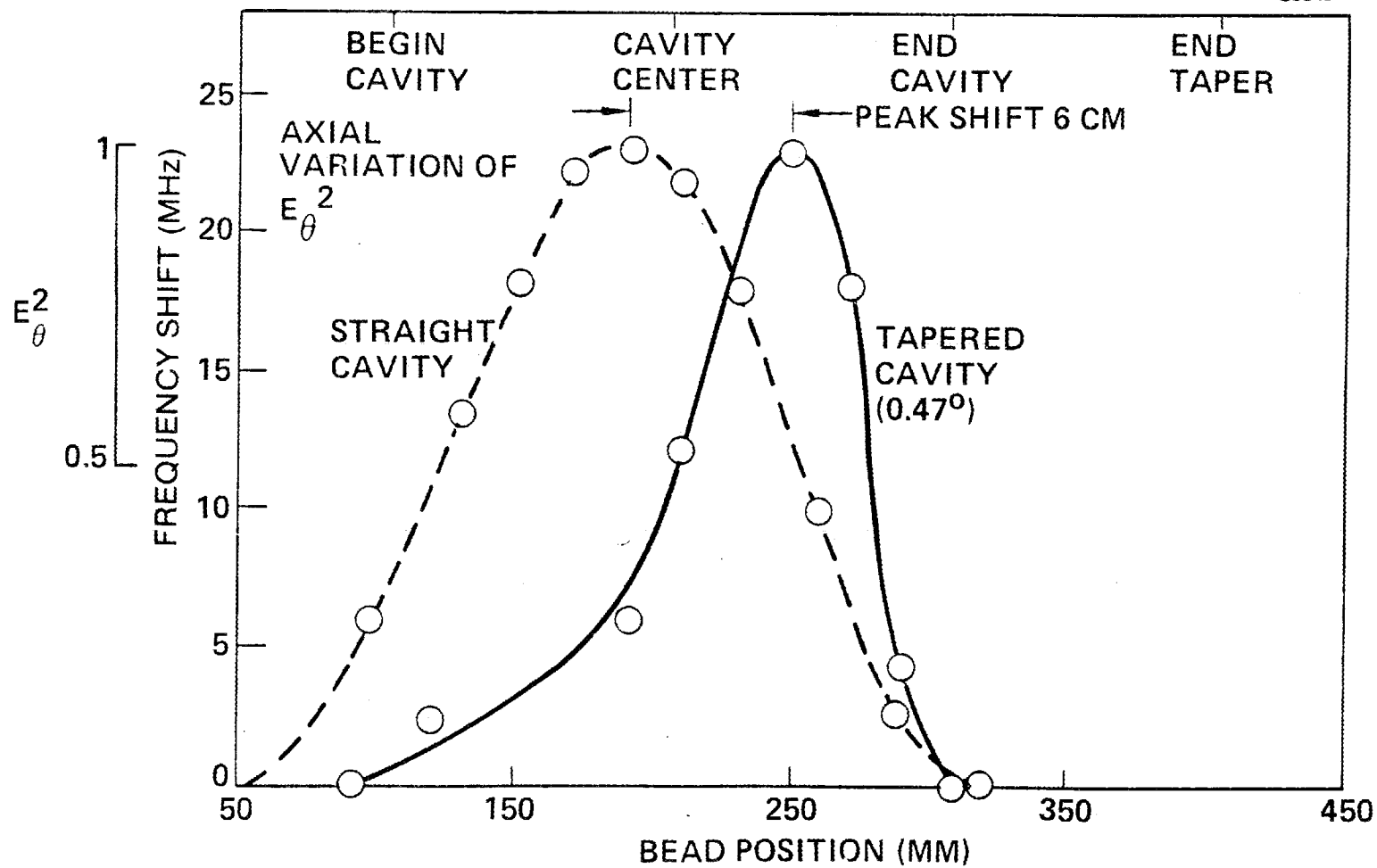


Figure 2.4.1-2 Gyrotron cold test TE₀₂₁ mode profile measurement.

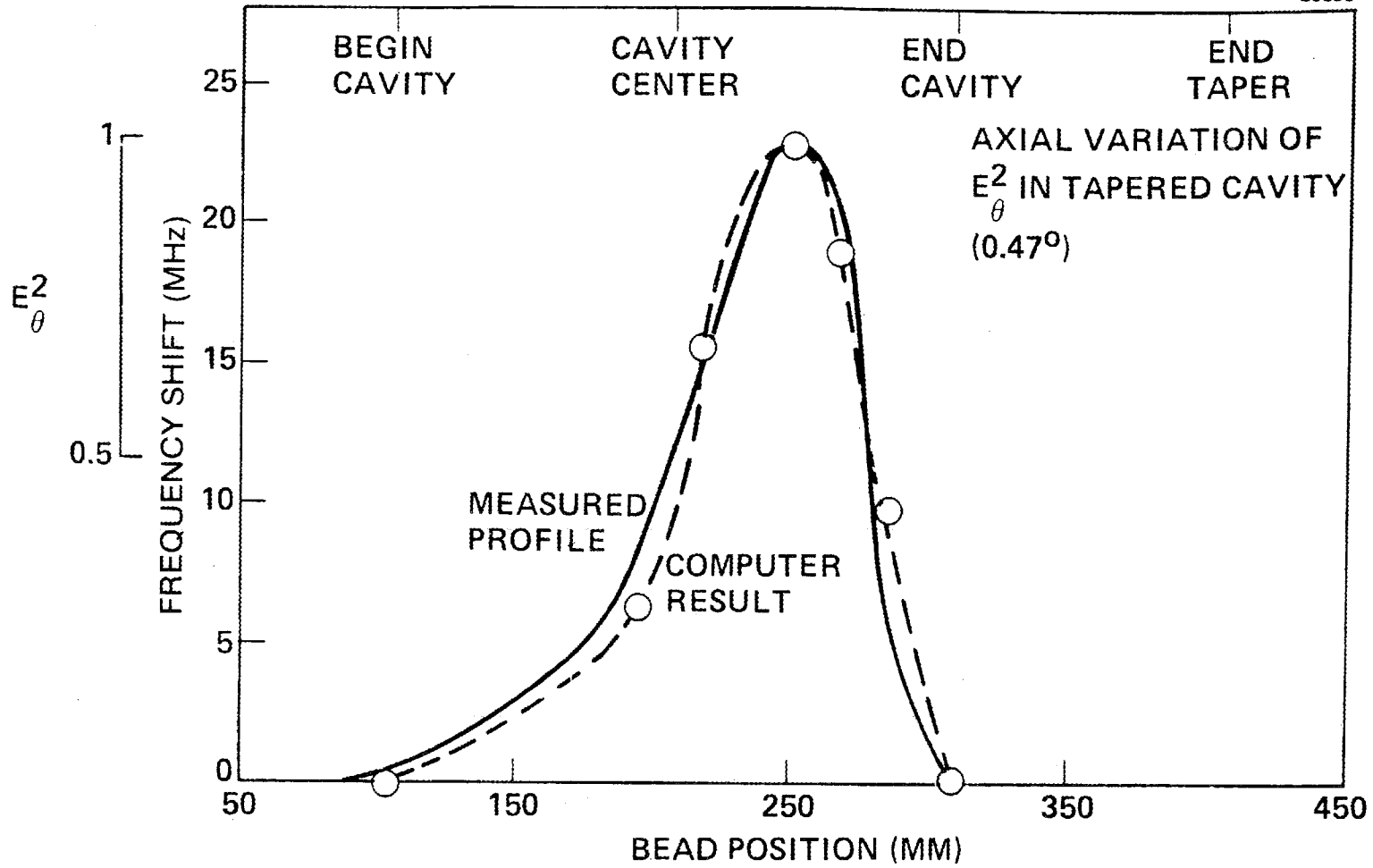


Figure 2.4.1-3 Measured profile vs computer result.

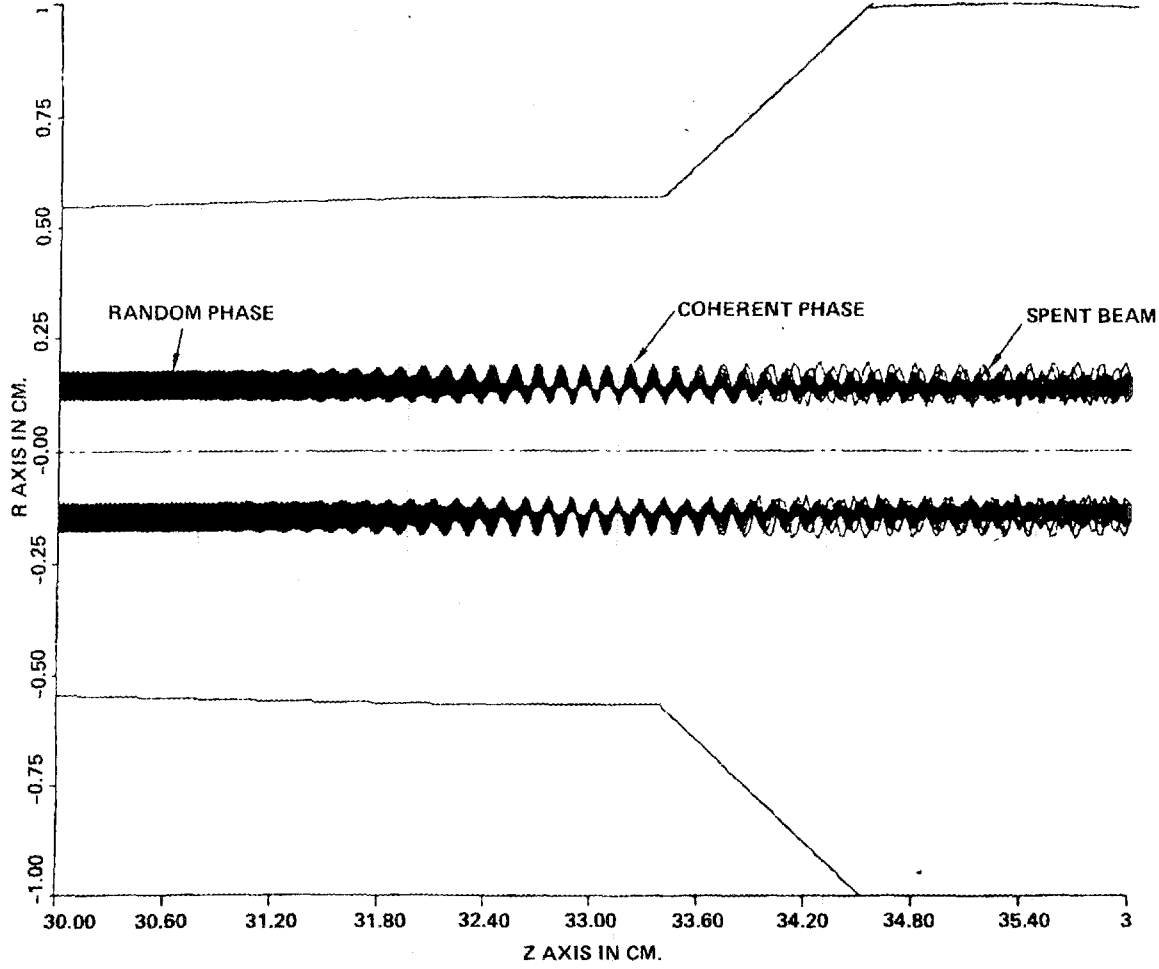
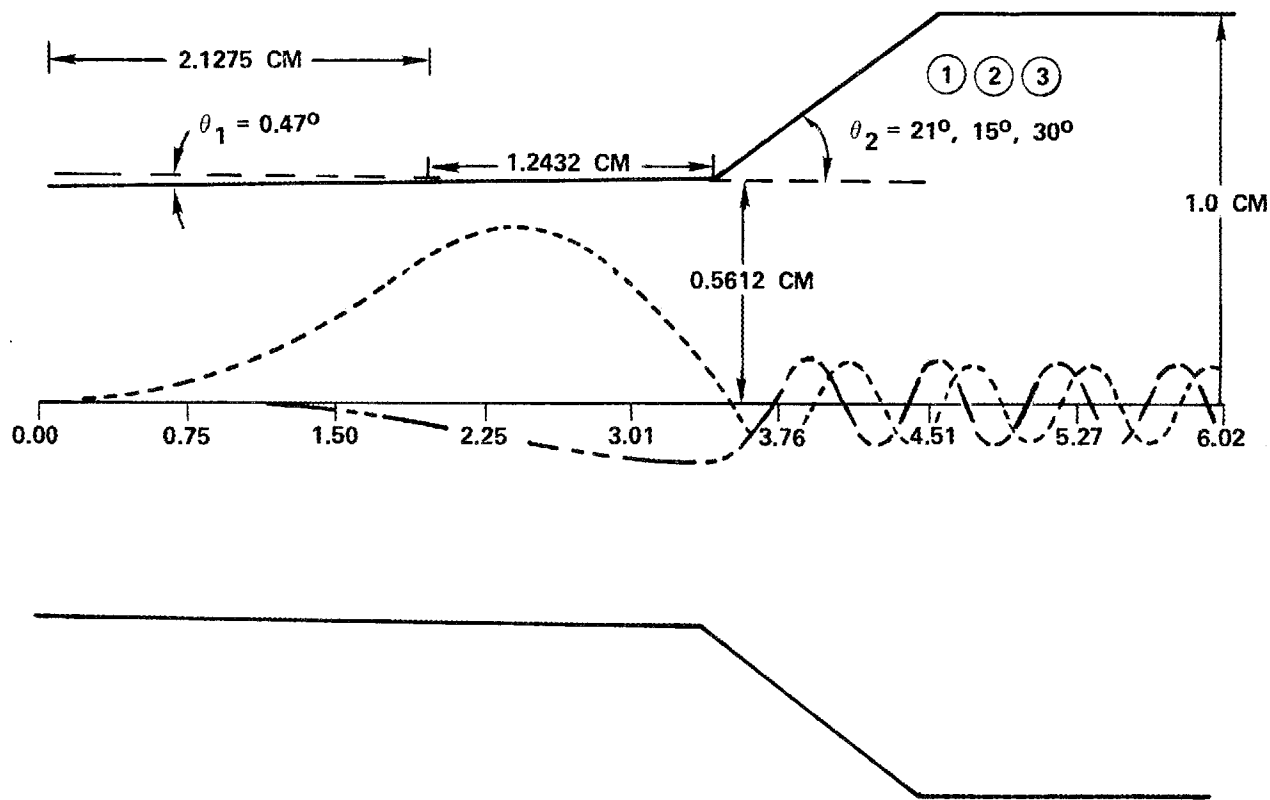


Figure 2.4.2-1 Phase bunching of hollow electron beams.



CAVITY Q = 464.345
 FREQ (GHZ) = 59.83828
 Q/MIN 0.822
 LMODE = 1.459
 KLOSS = 3469.8

~40% EFFICIENT
 NO MAGNETIC TAPER
 $V_{\perp}/V_{\parallel} = 1.5$
 $V_0 = 70\text{kV}$

Figure 2.4.2-2 Cavity configuration A.

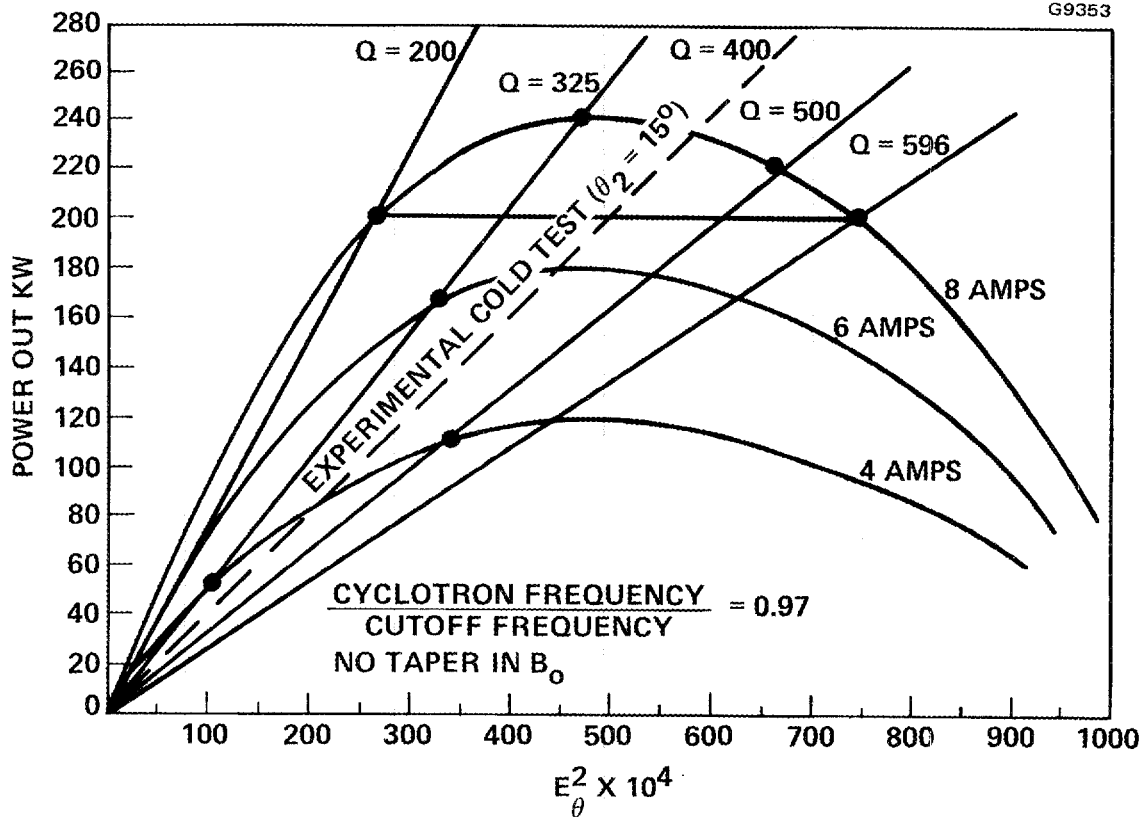


Figure 2.4.2-3 Efficiency analysis of configuration A.

10 GHz predicts a Q_{Ext} of approximately 400 for a 15° output taper and thus an output power of 240 kW at approximately 40% efficiency. Average CW wall loading on the cavity would be about 600 watts/sq. cm. Magnetic tapering for this cavity does not seem to greatly increase the predicted output power. Cavity #4 which has no input taper was ordered as a "control" cavity to be used in the cold test measurements at 60 GHz.

Cavity Configuration B

The dimensions of cavity #5 are shown in Figure 2.4.2-4. It is longer than the first cavity set (ratio of length to radius 7.46:1), and has an input taper angle of 1.04° giving a very sharp mode profile. This cavity is to operate optimally in the 7% tapered magnetic field, and is predicted to deliver an output power of at least 200 kW for any Q_{Ext} between 203 and 785 (Figure 2.4.2-5). Present cold test data predicts a Q_{Ext} of 620 for a 15° output taper and thus an output power of 230 kW at 40% efficiency. A 10% output taper angle is predicted to have a Q_{Ext} of 553 with an output power of 240 kW. Average CW wall loading on this cavity would be about 800 watts/sq cm. This cavity can give the same output power as those of the first set, but with higher Q values. This would allow for better mode separation, greater cavity isolation, and lower starting thresholds. It would also operate more effectively at degraded beam parameters, an important consideration for the "first" gyrotron device. The disadvantage for ultimate CW operation is that the higher Q_{Ext} results in greater power dissipation on the walls.

2.4.3 Threshold Analysis

Figure 2.4.3-1 shows the minimum starting currents vs magnetic mistuning for initially exciting the cavity and illustrates that the region of optimum efficiency occurs quite close to the edge of the operating region at 10 amps. This is a potential problem for pulsed operation.

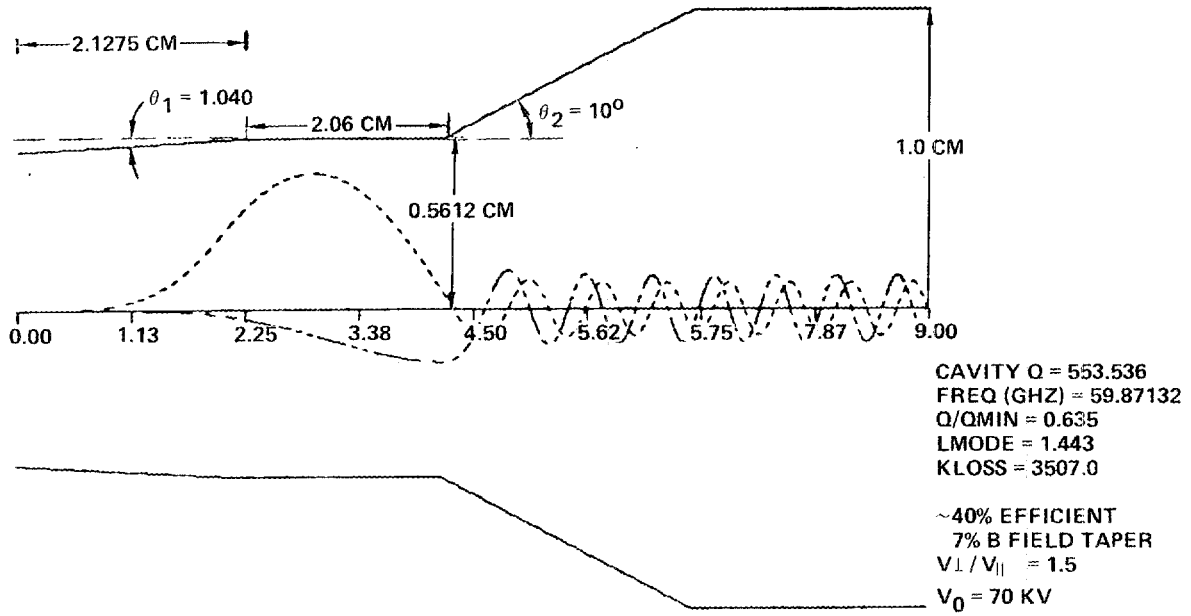


Figure 2.4.2-4 Cavity configuration B.

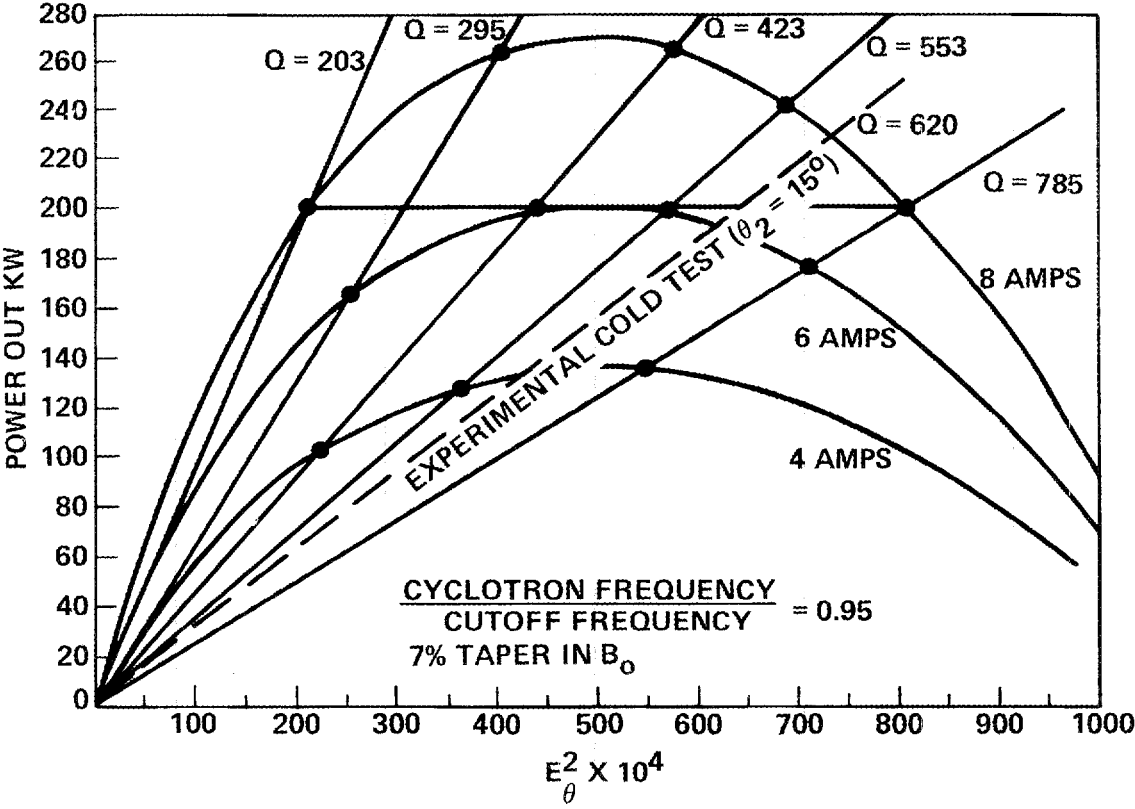


Figure 2.4.2-5 Efficiency analysis of configuration B.

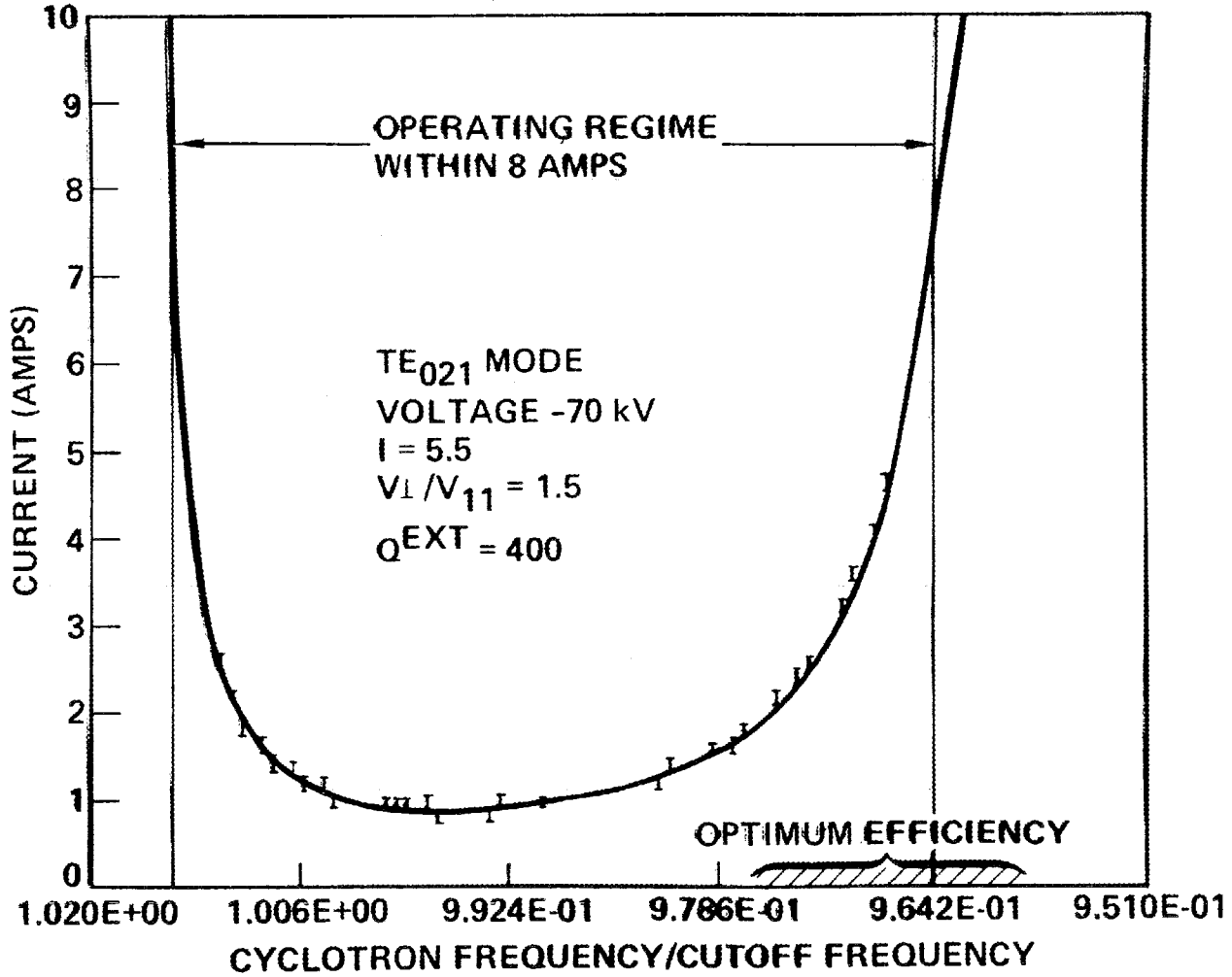


Figure 2.4.3-1 Start-up threshold analysis.

2.4.4 Final Cavity Design

The final choice of cavity for the first gyrotron device will await final cold tests at 60 GHz of cavities 1 through 5.

2.5 917H (CW) COLLECTOR

The mechanical design of the collector for the first experimental gyrotron was completed during this quarter. The electrical design was based on allowing the spent beam to spread along the naturally decaying magnetic field lines of the superconducting solenoid, i.e., no auxillary coils or magnets were used to spread the beam. The power density at which the spent beam impacts on the collector walls is dependent upon the diameter of the collector chosen. For a 3.5" I.D. collector, the predicted power density reaches 800 W/cm^2 at several points in the beam impact area.¹ Because this high power density is approaching the upper limit of power densities which can be sustained on a CW basis by water-cooling, it becomes advisable to have experimental verification of the beam location and power density.

One method of verifying beam location and power density is the measurement of X-rays emitted from the impact of the beam on the collector wall. This measurement should be made as close to the impact area as possible in order to avoid detection of diffracted X-rays from other impact areas within the collector. This implies that the collector for the first gyrotron should be constructed without cooling, and with as thin a wall thickness as structurally possible.

The design of the S/N 1 collector will employ a wall thickness of 0.2". The beam is expected to be contained within a 3.5" ID collector section which is 23" long. At the extremities of this straight section, an insulating choke has been devised which contains the RF within the 3.5" guide, but permits detection of beam current separate from other tube subassemblies. At the gun end of the straight collector section, the anode drift region, cavity and up-taper are electrically tied together. At the output end of the straight

collector section; the down taper, pump-out assembly and window are electrically tied.

A method of maintaining concentricity of ± 0.001 " through adjacent collector sections has been designed into the insulating choke.

2.6 919H (100 ms) COLLECTOR

The 100 ms tube needs only to withstand 2% duty operation, plus the accompanying effects of long-pulse thermal stresses. A preliminary analysis from the CW collector trajectory plot¹ shows that for a 1" diameter collector, the beam would collect over a 12.7 cm length in a region between 72 and 85 cm from the nose of the cathode. This comprises an area of 101 cm^2 for a worst case beam power of 560 kW peak. At 2% duty, the average power density is 110 watts/cm^2 , which is considered more than adequate. The peak heating effects however are an unknown at this time, and will be investigated further through a transient heat analysis for collector sizes of 1" to 2.5" diameter.

2.7 917H CW OUTPUT WINDOW

The preliminary design of an output window for the CW gyrotron has been completed. This window will actually use two windows with a surface cooling dielectric flowing between them.³ Edge-cooling of the windows will be accomplished with water. A functional representation of this double window configuration is shown in Figure 2.7-1.

A computer code has been programmed to evaluate the VSWR obtained from the double disc window design. This code permits rapid evaluation of window thickness and gap spacing between windows for the TE_{02} mode. Representative output plots from this window evaluation code are shown in Figures 2.7-2 and 2.7-3 for two window thicknesses ($\approx 3/2 \lambda_g$). It can be seen from these figures that the effect of larger gap spacings is to decrease the pass band slightly and lower the center frequency. The pass band itself is only about 1% at a VSWR of 1.25:1.

It is desirable to explore methods of increasing the pass band of the double disc configuration, by evaluating asymmetric double discs, and by exploring variations in wall diameter. In view of the very narrow bandwidth, it may be necessary to re-evaluate the feasibility of thinner windows with thicknesses of the order of λ_g .

Mechanically, further effort is required to refine this design, and completion is expected in the next quarter.

2.8 919H (100 ms) OUTPUT WINDOW

Since the average heat dissipation due to RF in 100 ms is not as severe as in the CW window, a single disc window will be employed. Figure 2.8-1 illustrates the calculated pass band for a single $3/2 \lambda_g$ window (using the double disc design code, with ϵ_R of the second window equal to 1.0). The bandwidth of the single disc is approximately twice that of the double disc, or about 2%. It should be possible to consider windows with thicknesses of the order of λ_g for the 100 ms tube, with little impact on window stress integrity.

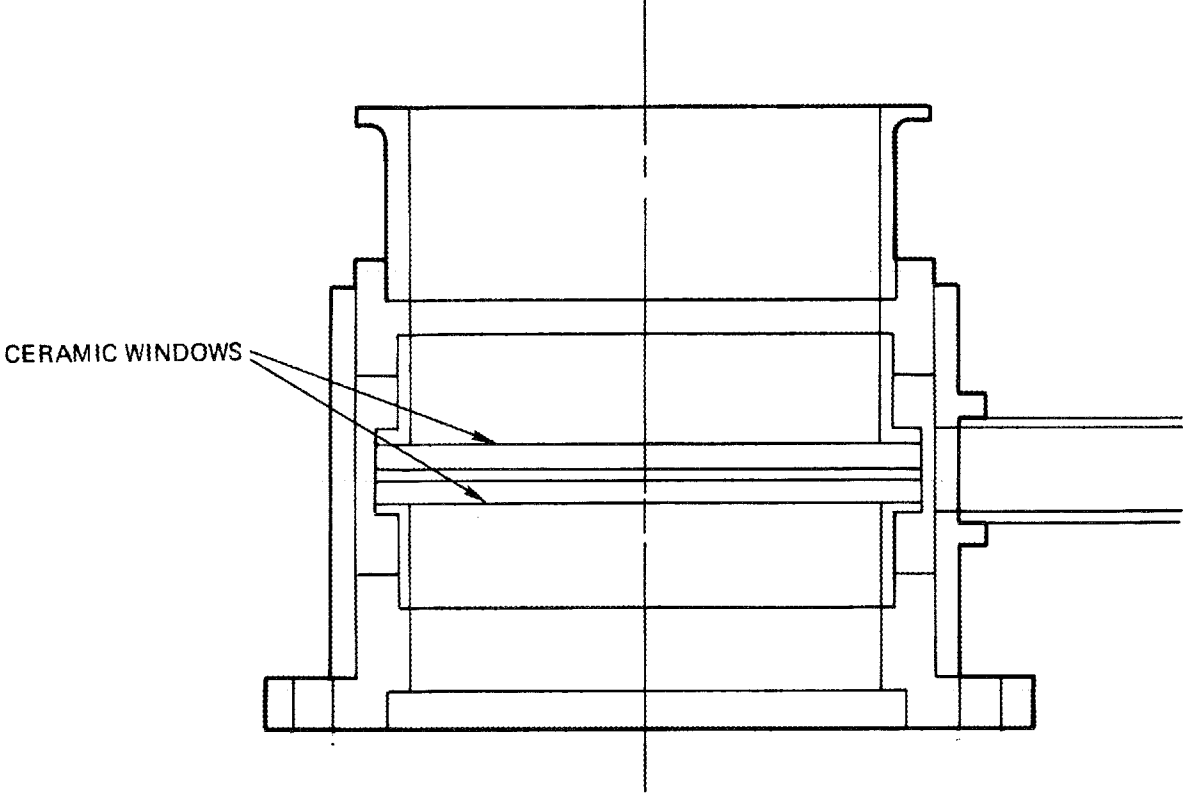


Figure 2.7-1 Double-Disc Window - preliminary sketch.

HUGHES DOUBLE DISC WINDOW DESIGN

BEG CERAMIC THICKNESS = 0.1170 INCHES

- GAP SPACING = 0.0310 _____
- GAP SPACING = 0.0340 _____
- GAP SPACING = 0.0370 _____
- GAP SPACING = 0.0400 _____
- GAP SPACING = 0.0430 _____
- GAP SPACING = 0.0460 _____

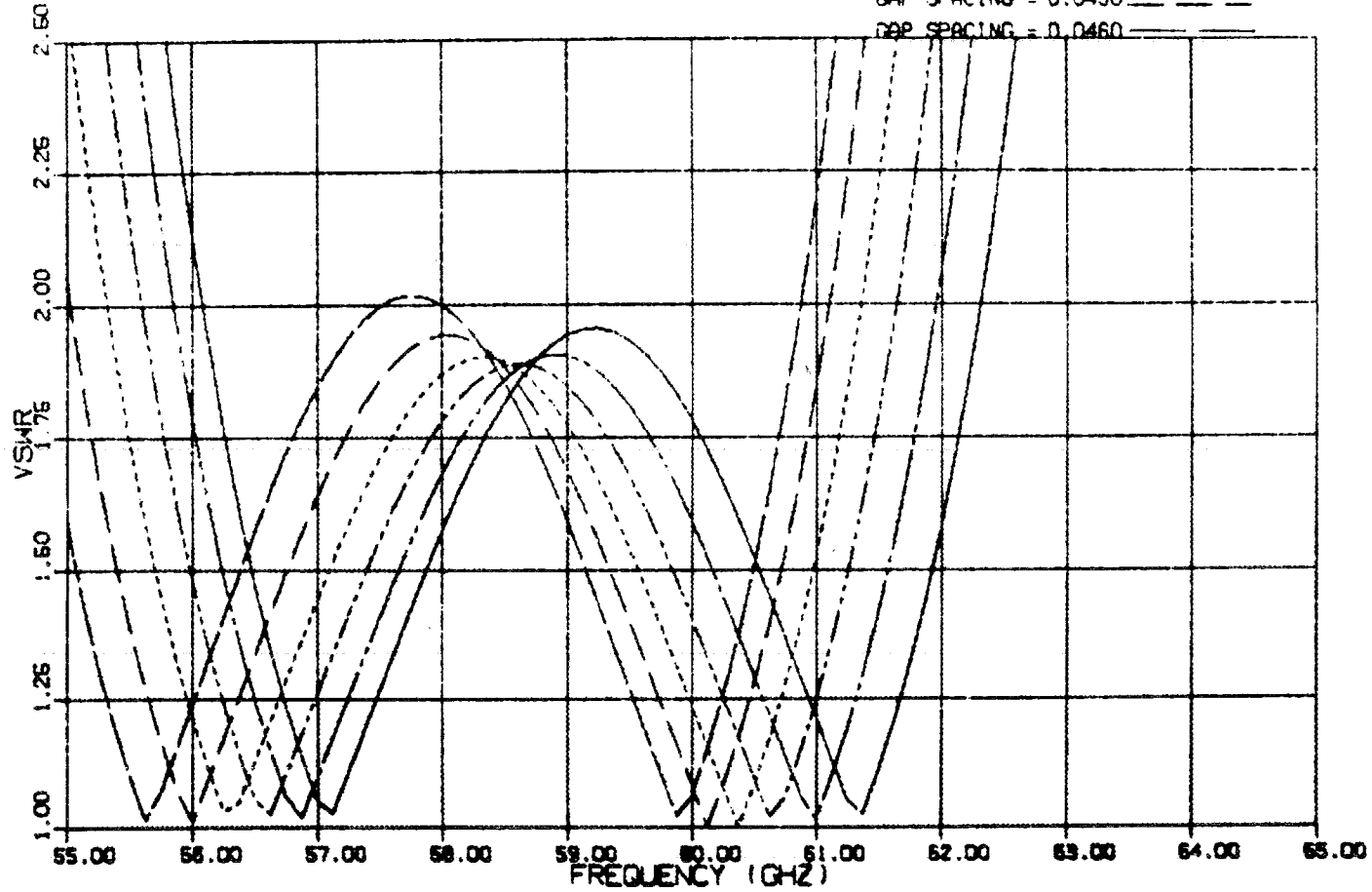


Figure 2.7-2 Calculated VSWR of double disc window, with dielectric coolant in the gap between windows. (Window thickness = 0.117").

HUGHES DOUBLE DISC WINDOW DESIGN

BEC CERAMIC THICKNESS = 0.1180 INCHES

- GAP SPACING = 0.0310 _____
- GAP SPACING = 0.0340 _____
- GAP SPACING = 0.0370 _____
- GAP SPACING = 0.0400 _____
- GAP SPACING = 0.0430 _____
- GAP SPACING = 0.0460 _____

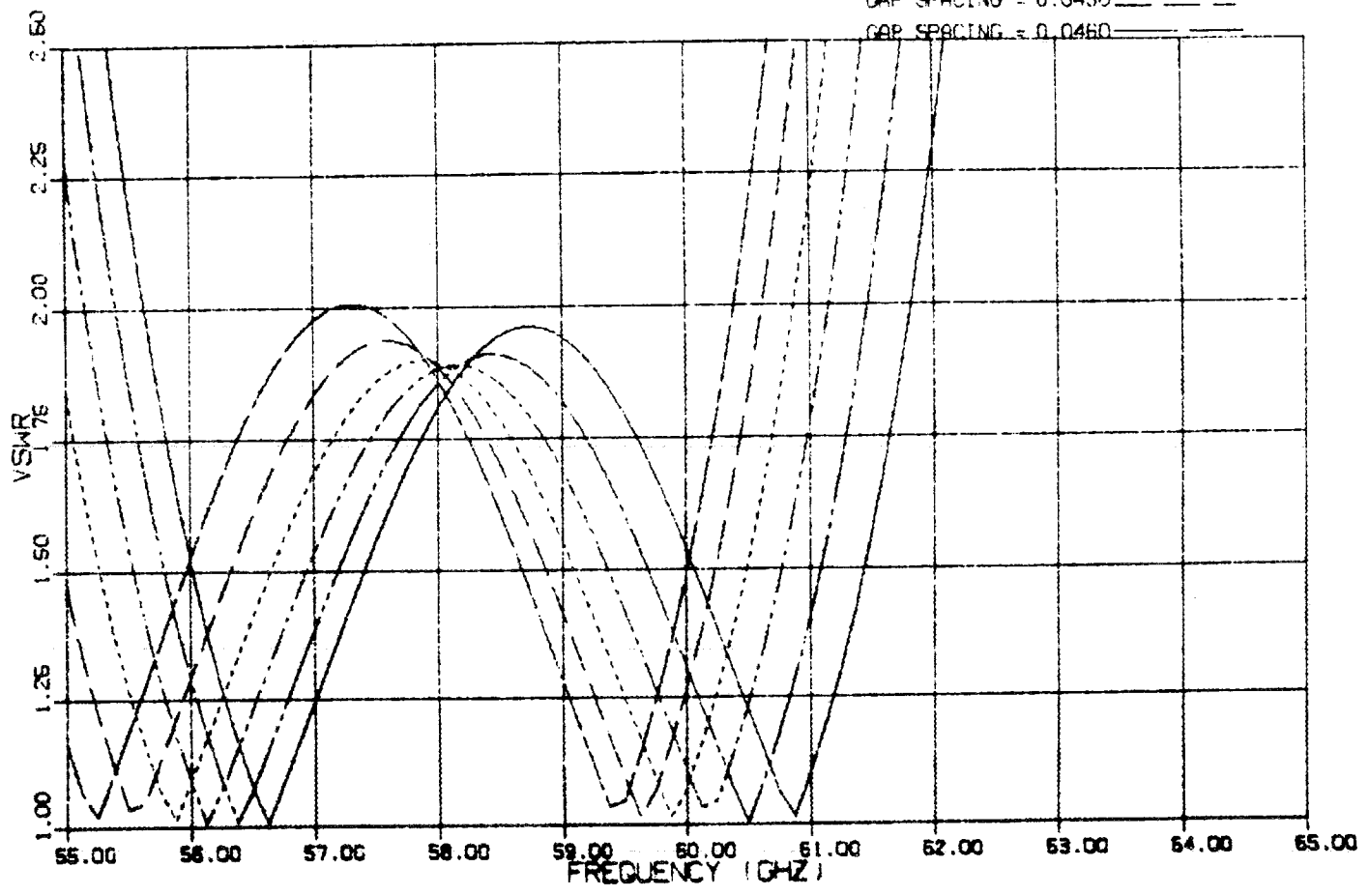


Figure 2.7-3 Calculated VSWR of double disc window, with dielectric coolant in the gap between windows. (Window thickness = 0.118").

HUGHES DOUBLE DISC WINDOW DESIGN

BE0 CERAMIC THICKNESS = 0.1140 INCHES

GAP SPACING = 0.0000 _____

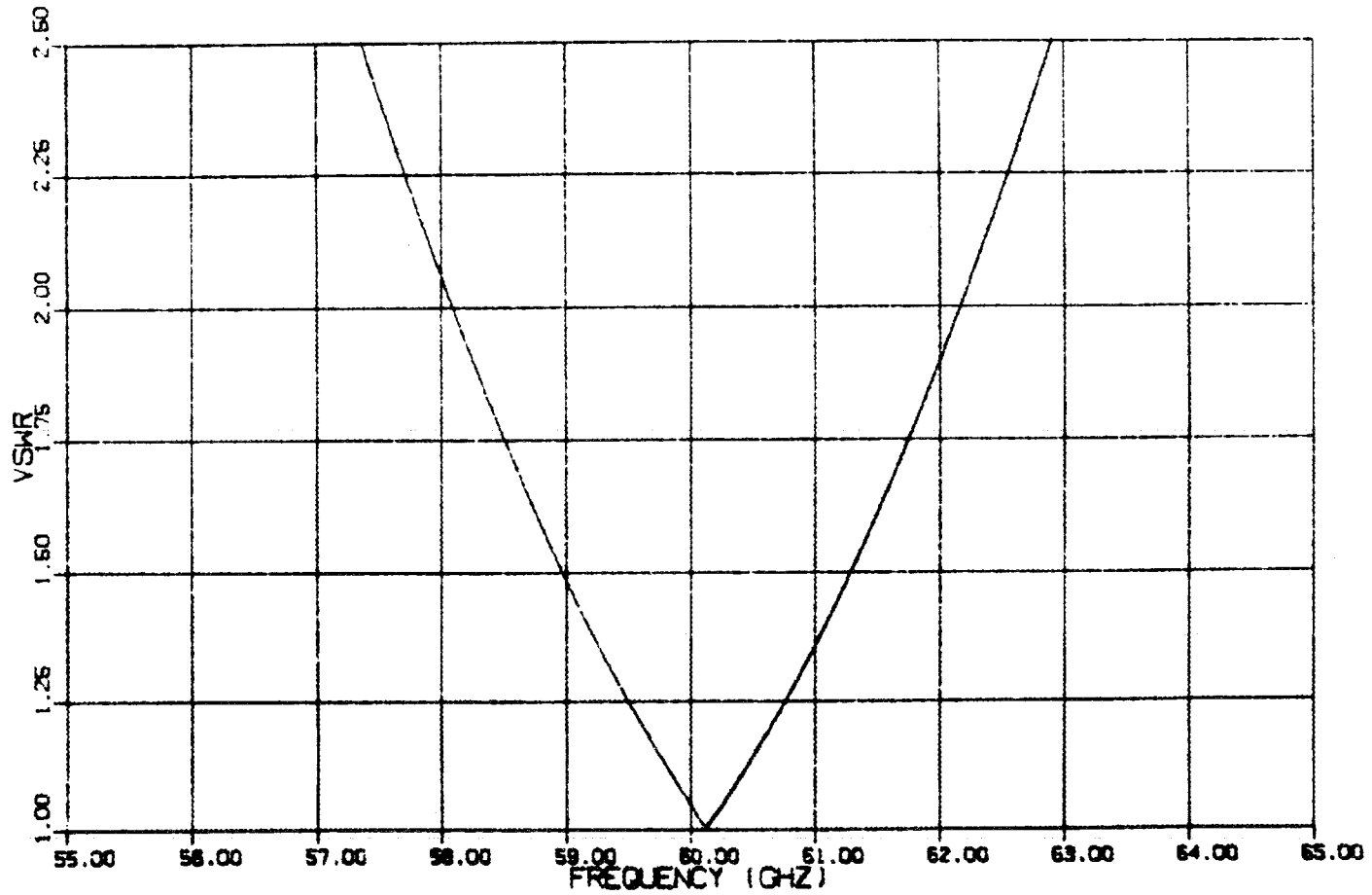


Figure 2.8-1 Calculated VSWR of single BeO window, no gap.

The mechanical design of the single disc window has been completed, and is shown in Figure 2.8-2. BeO discs have been ordered and are expected to be received in December 1980.

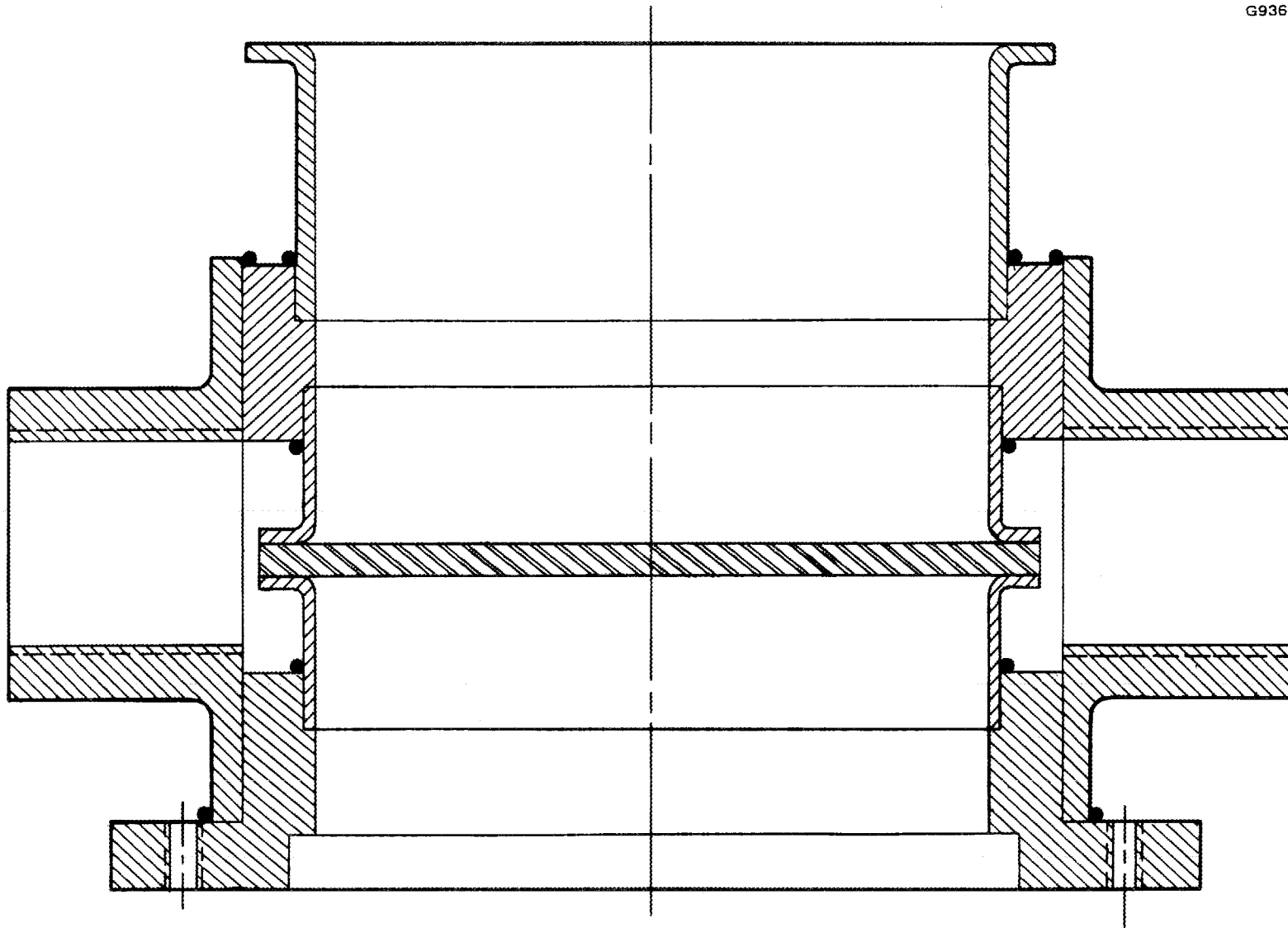


Figure 2.8-2 Mechanical design of single disc window.

2.9 POWER SUPPLIES

It is planned to use three supplies for testing the first gyrotrons:

- A modified cathode-pulsed supply with a 20 μ s, 2% duty capability at 70 kV max.
- A DOE-furnished supply, used on JFT-2, with 100 μ s to 100 ms, 1% duty at voltages up to 90 kV.
- A DOE-furnished supply, used at the Kwajalein Missile Range for the Missile Site Radar (MSR), with a 3 MW CW capability at 150 kV.

2.9.1 Short Pulse Power Supply

This supply is currently rated at 65 kV max. Modifications are underway to upgrade the supply for long term 70 kV operation. A compensated resistive divider network will be added to the supply in order to provide a continuously variable mod-anode voltage, from 0 to 35 kV with respect to the cathode. This supply will be used to obtain diagnostic data at low duty, less than 1%, immediately after the tube is pinched-off.

2.9.2 Medium Pulse Power Supply

This supply was constructed specifically for operation of a Varian 28 GHz, 40 ms pulse gyrotron at 80 kV. The supply is currently in operation in Japan on JFT-2, and is expected to be shipped to Hughes in April 1981. No modifications other than reassembly are anticipated. This supply will provide a 100 ms pulse capability in time for the required demonstration by December 31, 1981.

2.9.3 CW Power Supply

The MSR power supply was disassembled, packaged and shipped to Hughes from Kwajalein as part of the effort under this gyrotron program. Some damage was

inflicted during trans-shipping at Honolulu, wherein a portion of the capacitor bank was severely damaged. However, the number of capacitors ruined compared to the total capacitance of the supply is small, and it is believed that normal operation can be achieved without replacing the damaged capacitors.

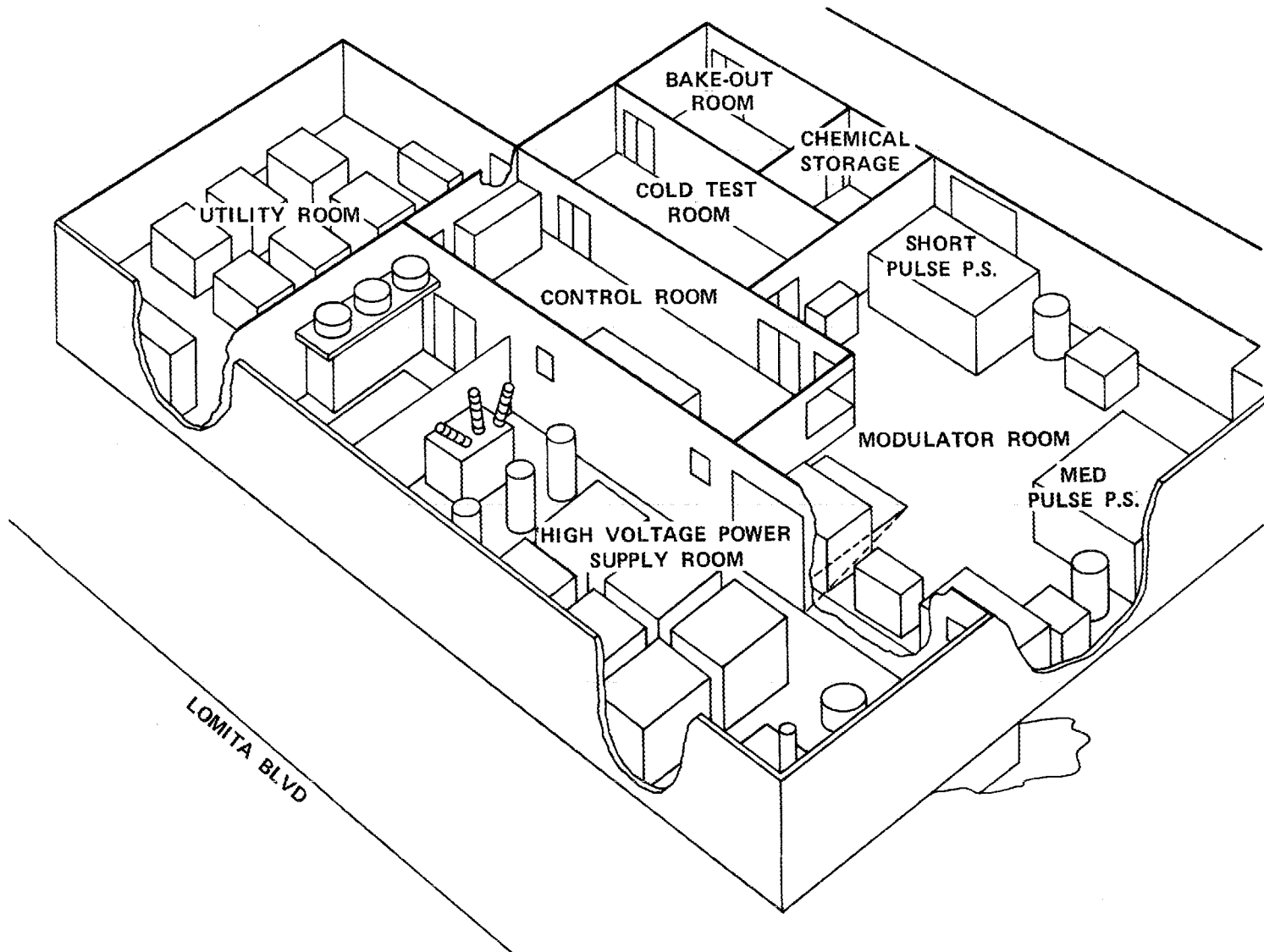
The disassembled MSR supply, including heat exchangers, pumps and water purification system were placed in storage at Hughes until such time that funding will permit reassembly.

In order to use the MSR supply in conjunction with the gyrotron, a modulator must be constructed which provides a mod-anode voltage and the ability to pulse the gyrotron for periods greater than 100 ms, including 30 seconds to CW.

2.10 GYROTRON FACILITY

Approximately 9000 sq. ft. of space is being provided for establishing a Gyrotron Laboratory in Building 237. This space will have adequate head-room for baking and vacuum processing gyrotrons up to 9' tall. (The 917H is just under 8' tall.). Since the gyrotron can be assembled from subassemblies using heli-arc welding, space has also been provided for cold test and final assembly.

A preliminary layout of the Gyrotron Facility is shown in Figure 2.10-1.

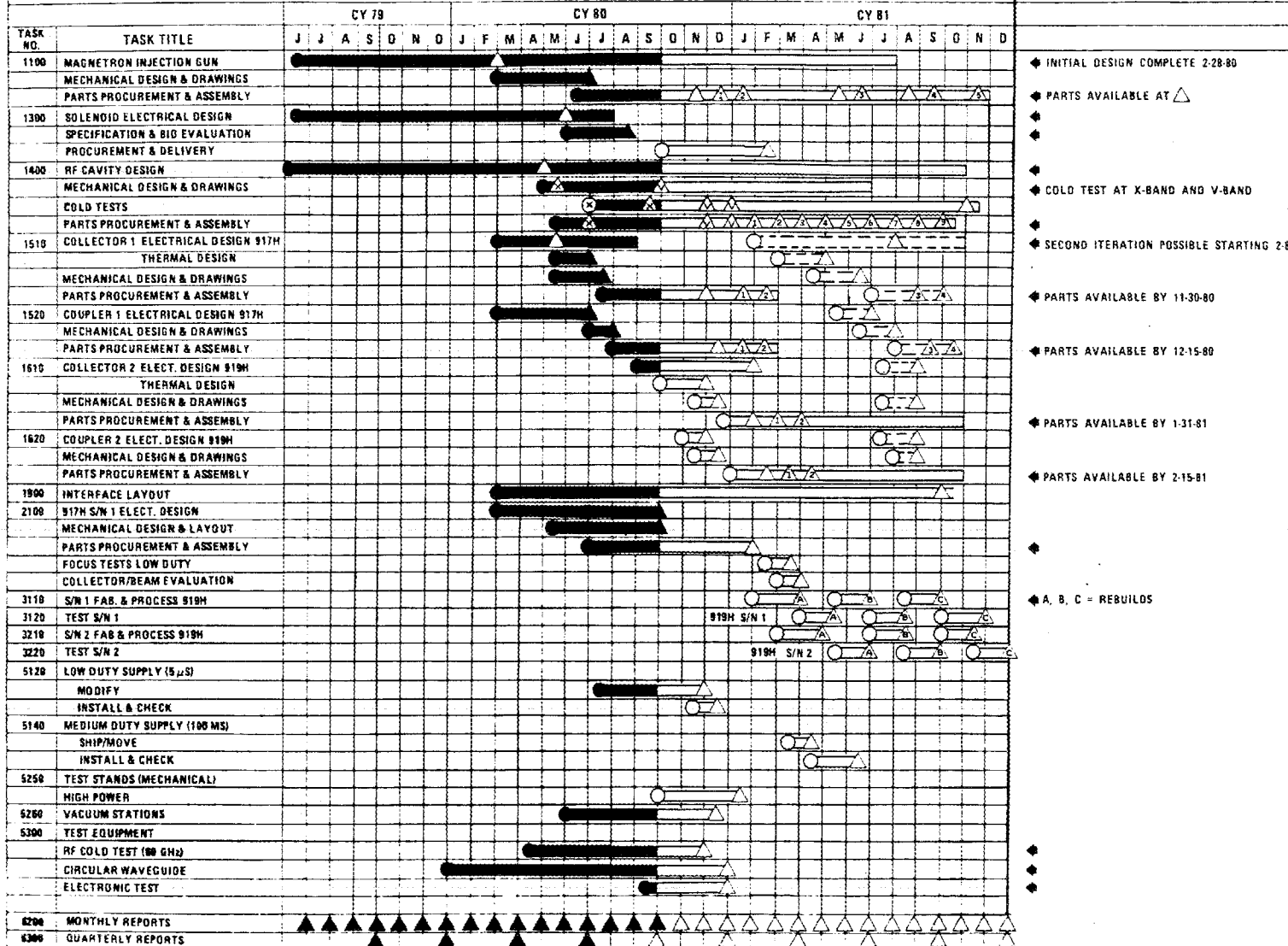


31

Figure 2.10-1 Preliminary facility layout.

3.0 SCHEDULE

3.1 A revised schedule, reflecting the effort required to demonstrate a .100 ms capability by December 31, 1981, is attached.



- ◆ INITIAL DESIGN COMPLETE 2-28-80
- ◆ PARTS AVAILABLE AT ▲
- ◆
- ◆
- ◆ COLD TEST AT X-BAND AND V-BAND
- ◆
- ◆ SECOND ITERATION POSSIBLE STARTING 2-81
- ◆
- ◆ PARTS AVAILABLE BY 11-30-80
- ◆
- ◆ PARTS AVAILABLE BY 12-15-80
- ◆
- ◆ PARTS AVAILABLE BY 1-31-81
- ◆
- ◆ PARTS AVAILABLE BY 2-15-81
- ◆
- ◆
- ◆ A, B, C = REBUILDS
- ◆
- ◆
- ◆

33

REFERENCES

1. J. J. Tancredi, M. Caplan, J. J. Sandoval, W. Weiss, Development Program for a 200 kW, CW Gyrotron, Quarterly Report No. 4, prepared by Hughes Aircraft Company for Oak Ridge National Laboratory under Contract W-7405-eng-26, ORNL/Sub-33200/4, April through June 1980.
2. K. W. Arnold, J. J. Tancredi, M. Caplan, K. W. Ha, D. N. Birnbaum, W. Weiss, Development Program for a 200 kW, CW Gyrotron, Quarterly Report No. 3, prepared by Hughes Aircraft Company for Oak Ridge National Laboratory under Contract W-7405-eng-26, ORNL/Sub-33200/3, January through March 1980.
3. F. Johnson, High Power R-F Window Study Program Quarterly Technical Note No. 1, prepared by Varian Associates for Rome Air Development Center under Contract AF 30(602)-2844, October 1962.

INTERNAL DISTRIBUTION

- | | |
|-----------------------|--|
| 1. A. L. Boch | 15. T. L. White |
| 2. J. L. Burke | 16-17. Laboratory Records Department |
| 3. R. J. Colchin | 18. Laboratory Records, ORNL-RC' |
| 4-7. H. O. Eason | 19. Y-12 Document Reference Section |
| 8. O. C. Eldridge | 20-21. Central Research Library |
| 9. R. P. Jernigan | 22. Fusion Energy Division Library |
| 10-12. C. M. Loring | 23. Fusion Energy Division Communications Center |
| 13. H. C. McCurdy | 24. ORNL Patent Office |
| 14. O. B. Morgan, Jr. | |

EXTERNAL DISTRIBUTION

25. R. A. Dandl, 1122 Calle De Los Serranos, San Marcos, CA 92069
26. R. J. DeBellis, McDonnell Douglas Astronautics Co., P.O. Box 516, St. Louis, MO 63166
27. J. F. Decker, Office of Fusion Energy, Department of Energy, APP, Rm. 219, GTN, ER-54, Washington, DC 20545
28. W. P. Ernst, Princeton University, Plasma Physics Laboratory, P.O. Box 451, Princeton, NJ 08540
29. W. Friz, AFAL/DHM, Wright Patterson AFB, OH 45433
30. T. Godlove, Particle Beam Program, Office of Inertial Fusion, Department of Energy, Mail Stop C-404, Washington, DC 20545
31. V. L. Granatstein, Naval Research Laboratory, Code 6740, Washington, DC 20375
32. G. M. Haas, Component Development Branch, Office of Fusion Energy (ETM), Department of Energy, Mail Stop G-234, Washington, DC 20545
33. G. W. Hamilton, Reactor Design, MFE Program, Lawrence Livermore National Laboratory, L6-44, P.O. Box 5511, Livermore, CA 94550
34. J. L. Hirshfield, Yale University, Department of Engineering and Applied Science, P.O. Box 2159, Yale Station, New Haven, CT 06520
35. T. James, Office of Fusion Energy, Department of Energy, Mail Stop G-234, Washington, DC 20545
36. K. Krause, Lawrence Livermore National Laboratory, P.O. Box 808/L-443, Livermore, CA 94550
37. H. Jory, Varian Associates, 611 Hansen Way, Palo Alto, CA 94303
38. J. V. Lebacqz, Stanford Linear Accelerator Center, P.O. Box 4349, Stanford, CA 94305
39. W. Lindquist, Electronics Engineering Department, Lawrence Livermore Laboratory, P.O. Box 808/L-443, Livermore, CA 94550
40. M. R. Murphy, Office of Fusion Energy (ETM), Department of Energy, ER-531, GTN, Washington, DC 20545
41. J. H. Pfannmuller, McDonnell Douglas Astronautics Co., c/o Oak Ridge National Laboratory, P.O. Box Y, Bldg. 9983-32, Oak Ridge, TN 37830
42. G. F. Pierce, 53 Lomond Drive, Inverness, IL 60067
43. B. H. Quon, TRW Defense & Space Systems, 1 Space Park, Bldg. R-1, Redondo Beach, CA 90278
44. M. E. Read, Naval Research Laboratory, Code 6740, Washington, DC 20375
45. D. B. Remsen, General Atomic Company, P.O. Box 81608, San Diego, CA 92138

46. T. Roemesser, TRW Defense & Space Systems, 1 Space Park, Bldg. R-1, Redondo Beach, CA 90278
47. G. Simonis, Harry Diamond Laboratory, 2800 Powder Mill Road, Adelphi, MD 20783
48. B. Stallard, Lawrence Livermore Laboratory, University of California, L-437, P.O. Box 808, Livermore, CA 94550
49. H. S. Staten, Office of Fusion Energy (ETM), Department of Energy, Mail Stop G-234, Washington, DC 20545
50. P. Tallerico, AT-1 Accelerator Technology Division, Los Alamos Scientific Laboratory, Mail Stop 817, P.O. Box 1663, Los Alamos, NM 87545
51. R. J. Temkin, National Magnet Laboratory, Massachusetts Institute of Technology, Cambridge, MA 02139
52. Director, U.S. Army Ballistic Missile Defense Advance Technology Center, Attn.: D. Schenk, ATC-R, P.O. Box 1500, Huntsville, AL 35807
- 53-54. Department of Energy Technical Information Center, Oak Ridge, TN 37830
55. RADC/OCTP, Griffiss AFB, NY 13441
56. Office of Assistant Manager for Energy Research and Development, Oak Ridge Operations Office, Department of Energy, Oak Ridge, TN 37830